Slope-velocity-equilibrium and evolution of surface roughness on a stony hillslope

Mark A. Nearing[1], Viktor O. Polyakov[1], Mary H. Nichols[1], Mariano Hernandez[1], Li Li[2], Ying Zhao[2], Gerardo Armendariz[1]

[1]USDA-Agricultural Research Service, Southwest Watershed Research Center, Tucson, AZ, 85719, USA
[2]School of Natural Resources and the Environment, University of Arizona, Tucson, AZ, 85705, USA

Correspondence to: Mark A. Nearing (mark.nearing@ars.usda.gov)

Abstract. Slope-velocity-equilibrium is hypothesized as a state that evolves naturally over time due to the interaction between overland flow and surface morphology, wherein steeper areas develop a relative increase in physical and hydraulic roughness such that flow velocity is a unique function of overland flow rate independent of slope gradient. This study tests this hypothesis under controlled conditions. Artificial rainfall was applied to 2 m by 6 m plots at 5%, 12%, and 20% slope gradients. A series of simulations were made with two replications for each slope, with measurements of runoff rate, velocity, rock cover, and surface roughness. Velocities measured at the end of each replication were a unique function of discharge rates, independent of slope gradient or rainfall intensity. Physical surface roughness was greater at steeper slopes. The data clearly showed that there was not a unique hydraulic coefficient for a given slope, surface condition, or rainfall rate, with hydraulic roughness greater at steeper slopes and lower intensities. This study supports the hypothesis of slope-velocity-equilibrium, implying that use of hydraulic equations, such as Chezy and Manning, in hillslope scale runoff models is problematic because the coefficients vary with both slope and rainfall intensity.

1 Introduction

Hillslopes in semi-arid landscapes evolve in various ways, one of which is the formation of surface roughness through soil erosion. As surface erosion occurs, surficial material is preferentially detached and transported according to particle size, detachability, and transportability. This process results in a hillslope with an erosion pavement that is characterized by greater surface rock cover than that of the original soil. An erosion pavement is "a surface covering of stone, gravel, or coarse soil particles accumulated as the residue left after sheet or rill erosion has removed the finer soil" (Shaw, 1929). Once formed, the erosion pavement acts as a protective cover against erosive forces, which reduces subsequent rates of soil erosion. Erosion pavements are analogous to desert pavements formed in arid regions by wind erosion.

Because erosion potential is greater with steeper slope, the rock cover resultant from the process of erosion pavement formation along the hillslope profile is positively correlated to slope steepness in many semi-arid environments, which has been documented in previous studies at the USDA-Agricultural Research Service's Walnut Gulch Experimental Watershed (Walnut Gulch hereafter) in south-eastern Arizona. Simanton et al. (1994) measured rock cover at 61 points along 12 different

catenas at Walnut Gulch, with slopes at points ranging from 2 to 61%. They found that rock fragment cover (>0.5 cm), R_{fc} (%), was a logarithmic function of slope gradient, S (%), with greater rock cover associated with steeper parts of the hillslopes.

They also measured the rock fragments in the upper 50 mm of soil and found that total rock fragments in the soil was also correlated to slope steepness. Nearing et al. (1999) measured surficial rock content at the Lucky Hills site in Walnut Gulch on a range of slope gradients and also found a positive logarithmic relationship between rock cover and slope. Poesen et al. (1998) also reported a positive correlation between rock cover and slope gradient for a semiarid site in Spain. van Wesemael et al. (1996) also looked at hillslopes in the field in south-eastern Spain and found that both rock cover and surface roughness increased as a function of slope gradient.

Increased rock cover is associated with increased hydraulic friction because the rocks act as form roughness elements in shallow flow and thus create drag, and reduced soil erosion, both because the rocks protect the surface and because they dissipate flow energy. Rieke-Zapp et al., (2007) conducted a laboratory study with a soil mixed with rock fragments to investigate the evolution of the surface as the material was eroded by shallow flow. They measured flow rates and velocities, surface morphology (with a laser scanner), erosion (by measuring sediment concentrations from runoff samples), and rock cover change. The soil was a relatively highly erodible silt loam, which formed rills in the flume. They reported that rock fragment cover increased with time during the experiments, resulting in an armouring effect that greatly reduced erosion rates as flow energy was dissipated on the rocks. They also found that for treatments with no initial rock content in the soil, flows were narrower and formed headcuts that also acted to reduce flow velocity when rocks were not present. They reported that the addition of only small amounts of rocks in the initial soil matrix greatly reduced erosion rates compared to the soil with no rocks. Rill widths were greater for treatments with more rock.

The most common methods for mathematically describing the velocity of runoff on a hillslope are with either the Chezy (or the related Darcy-Weisbach) or Manning equations (e.g., Graf 1984; Govers et al., 2000; Hussein et al., 2016). Both of these equations relate flow velocities to slope gradient and flow rate using a hydraulic roughness factor, which is generally considered to be related to the morphological roughness of the surface in some way. The equations work well for fixed channel or rill beds (flow surfaces), but this approach when applied to eroding rills is problematic. In an eroding rill the flow interacts with the bed to change the surface morphology, which also changes the hydraulic roughness, and hence flow velocity. In other words, there exists a dynamic feedback between the rill flow and the bed morphology on an eroding surface (see, e.g., Lei et al., 1998).

The dynamic feedback between flow, bed morphology, and erosion was discussed in a hypothesis testing study conducted by Grant (1997), in a broad way, from the perspective of mobile-bed river channels. Grant's hypothesis stated that "*in mobile-bed river channels, interactions between the channel hydraulics and bed configuration prevent the Froude number from exceeding one for more than short distances or periods of time*." In other words, when the kinetic energy of flow exceeds the gravitational energy, flow instability is created that results in "*rapid energy dissipation and morphologic change*" that counteracts flow acceleration and "*applies the 'brake' to flow acceleration.*" Grant argues that this system is consistent with the concept of energy minimization, because flow rate relative to flow energy is maximized at critical flow. Grant suggests

that this general mechanism may be applicable in channels ranging from boulders to sand bed streams, with structures including step-pools and antidunes. It has also been suggested that supercritical flow is necessary for the development of headcuts in upland concentrated flows (Bennett et al., 2000; Byron, 1990), which then act to retard flow velocities.

Govers (1992) used a compilation of data from laboratory experiments on eroding rills and determined that the measured flow velocities were independent of slope and related well to flow discharge alone:

$$v = 3.52\ Q^{0.294}\ (r^2 = 0.73,\ n = 408), \quad (2)$$

where v is the average flow velocity (m s^{-1}) and Q is the rill discharge ($m^3\ s^{-1}$). Nearing et al. (1997) also reported velocity independence to slope from laboratory and field experiments in rills. Takken et al. (1998) found that equation (2) was valid only when conditions allowed for free adjustment of the rill bed geometry by erosion, either due to headcut formation or increased rock cover. Note that, for example, Foster et al. (1984) conducted velocity studies on a full-scale, fixed-bed fiberglass model of a "rill" and found that velocity was related to slope steepness by the power of 0.48. Flow velocity was more sensitive to slope steepness than it was to flow rate for the fixed bed rill in that experiment. Correspondent interrelationships between flow velocities, flow rates, and slope gradients have not been investigated for interrill or sheet flow conditions.

Nearing et al. (2005) hypothesized that stony hillslopes in the semi-arid environment evolve to a state of "slope-velocity-equilibrium". We define slope-velocity equilibrium as a state that evolves naturally over time due to the interactions between overland flow, erosion, and bed surface morphology, wherein steeper areas develop a relative increase in physical and hydraulic roughness such that flow velocity is a unique function of overland flow rate independent of slope gradient. Under these conditions runoff flow rates and velocities would increase approximately linearly down the slope under normal runoff conditions, independent of slope gradient. This hypothesis was based in part on a study of erosion rate estimations on two small, gaged watersheds at Walnut Gulch using ^{137}Cs inventories. They found that the spatial distribution of erosion rates estimated from the ^{137}Cs measurements were correlated to the surface rock fragment content, but were independent of slope gradients and curvature. They suggested that these results related to the processes of hillslope evolution, where the historic erosion of fine materials that occurred prior to the timespan covered by the measurement, determined the surface roughness that controlled the erosion rate during the timespan of measurement. In other words, they hypothesized that the steeper the slope is on the hillslope, the greater is the washing out of the fines and the rougher is the resultant surface. The rougher surface will reduce both overland flow velocity as well as erosion potential. The influence of surface roughness appeared to be the dominant control over the erosion, rather than slope gradient. They interpreted the dependence between erosion and rock cover and the independence of slope gradient influence over erosion rates, in terms of "slope-velocity equilibrium".

Given that the slope characteristics had been largely determined prior to the time period represented by the field experiment with the ^{137}Cs (Nearing et al., 2005), it is reasonable that more rock at a sampling point correlated to erosion less than would otherwise occurred between 1963 and 2004, which was the approximate time span representative of the erosion estimates. The energy (and hydraulic shear) of flow available for erosion and transport of sediment was reduced as a function

of increased hydraulic roughness of soil surface cover (rocks) because of the increased energy lost on the rougher surface (Nearing et al., 2001).

In this study we will investigate the development and hydrologic nature of slope-velocity equilibrium. We hypothesize that as the slopes evolve to a state of slope-velocity equilibrium through the process of preferential erosion of fines and resultant increase in surface roughness, flow velocity becomes independent of slope gradient. Rainfall simulation experiments were designed and conducted to test this hypothesis.

2 Materials and Methods:

2.1 Soil and instrumentation

The soil used in the experiment was Luckyhills-McNeal gravely sandy loam formed on deep Cenozoic alluvial fan. It contains approximately 52% sand, 26% silt, 22% clay and less than 1% organic carbon. The soil was collected from the top 15 cm layer on level ground in the Lucky Hills area of the Walnut Gulch Experimental Watershed (31.740502, -110.061935), mixed, and stored in a pile. The experiment was conducted in a 6 m by 2 m by 0.3 m pivoted steel box with adjustable (0 to 20%) slope.

Rainfall was delivered using a portable, computer-controlled, variable intensity rainfall simulator (Walnut Gulch Rainfall Simulator). The WGRS is equipped with a single oscillating boom with four V-jet nozzles that can produce rainfall rates ranging between 13 and 190 mm h^{-1} with variability coefficient of 11% across 2 by 6.1 m area. Kinetic energy of the simulated rainfall was approximately 204 kJ ha^{-1} mm^{-1}. Detailed description and design of the simulator is available in Stone and Paige (2003) and Paige et al. (2004). Prior to the experiment the simulator was positioned over the soil box and calibrated using a set of 56 rain gages arranged on the plot in rectangular grid. The simulator was surrounded with wind shields to minimize rain disturbance.

Runoff rate from the plot was measured using a V-shaped flume equipped with electronic depth gage and positioned at 4% slope. The flume was calibrated prior to the experiment to determine the depth to discharge relationship. Throughout the simulation timed volumetric samples of runoff were taken as a control of runoff rates.

Overland flow velocity was determined using a salt solution and electrical sensors at the end of the plot. Two liters of the solution were uniformly applied on the surface using a perforated PVC pipe placed across the plot. The application distances were 1.65, 3.5, 5.8 m from the outlet. Salt transport was monitored through electrical resistivity of the runoff water measured with sensors imbedded in the outlet flume. The data was collected at 0.37 s intervals with real time graphical output using LoggerNet3 software and CR10X3 data logger by Campbell Scientific. Peak values from the salt curve were used because they were consistently more reliable, and hence comparable, relative to computation of the centroid of the salt curve, which is sometimes used.

Surface rock cover was measured at 300 points on a 20 x 20 cm grid using a hand-held, transparent, size-guide held over the surface. A single point laser sliding along a notched rail placed across the plot and pointed down on the plot was used

to objectively identify the sample point locations. The technique ensured that surface rock was measured at the same points every time during the course of the experiment. The rocks were counted and classified by size: 0-0.5 (soil), 0.5-1, 1-2, 2-4, 4-8, 8-15, and >15 cm. Rock cover percentage was considered to be the percentage of points with rocks greater than 0.5 cm present.

Surface elevations were measured along three 2 m long transects oriented across the plot at 0.9, 2.9 and 4.9 m from the lower edge of the plot. Elevation points along these transects were measured at 5 mm intervals with at 0.2 mm vertical resolution using a Leica3 E7500i laser distance meter mounted on an automated linear motion system. The data was logged by a Bluetooth3 enabled mobile device using Leica1 software.

A photo of the experiment in progress is shown in the supplementary material.

2.2 Experimental procedure

The entire experiment included three treatments with soil slope gradients of 5, 12, and 20% with two replications for each treatment. A replication consisted of 3 (for 20% slope) or 4 (for 5% and 12% slope) individual rainfall simulations (a simulation is considered to be one continuous application of rainfall on the plot) that progressively increased from 1.5 to 5 hours. The reason for the increasing duration was expectation that over time the slope would evolve at a progressively slower rate. The 20% slopes were simulated only 3 times because they initially eroded more quickly, and the surface evolved more quickly, than did the other two slopes. In this paper we will use the words "treatment" to refer to the three slope gradients, "replication" to refer to one of the two sets of simulations performed on each slope, and "simulation" as the single application of rainfall, applied 3 to 4 times for each replication. A schematic example of the sequence of measurements can be found in the Supplementary information.

Prior to the experiment the soil was placed in the box and spread evenly in an approximately 20 cm layer. The box was positioned horizontally, covered with cloth to prevent splash, and low intensity rainfall (35 mm h^{-1}) was applied until the soil was wetted throughout. This ensured a relatively consistent moisture starting condition for each replication, and allowed for more rapid development of steady-state runoff with minimal erosion occurring before the first measurement of runoff velocity. After pre-wetting, the box was positioned at the target slope and protective cloth was removed.

The experimental procedure was as follows. Immediately before the first rainfall simulation of each replication, soil surface measurements (rock cover and laser elevation transects) were conducted. The first rainfall simulation of the replication started with 60 mm h^{-1} intensity. Flow rate was recorded and runoff samples collected throughout the simulation: more frequently on the rising and falling limbs of the hydrograph and then every 5 to 15 min depending on the total simulation duration. After runoff had reached steady state during simulation 1 of each replication, flow velocity was measured over three distances starting from the shortest. Flow rate was recorded and a runoff sample collected with every velocity measurement. Then the rainfall intensity was increased to 180 mm h^{-1} and velocity measurements repeated. The simulation continued for approximately one hour, after which velocities were measured again at high (180 mm h^{-1}) and low (60 mm h^{-1}) rainfall

intensities. Velocities at high (180 mm h^{-1}) and low (60 mm h^{-1}) rainfall intensities were measured at the beginning and end of simulation 1 and at the end of each subsequent simulation. Similarly, soil surface measurements of roughness and rock cover were measured prior to the first simulation and after every simulation.

When all simulations of a replication were completed the top soil layer in the box was removed and replaced.

2.3 Data Analyses

Statistical analyses were performed using SAS and Excel. Differences reported in the paper are based on P=0.05 or lower. The datasets generated during the current study are available from the corresponding author on reasonable request.

Values of Chezy C and Manning's n were calculated using the standard equations for each and the measured velocities and known slopes. Hydraulic radii were calculated from the measured average discharge and flow velocities.

Relationships involving rock cover and random roughness with each other and with cumulative runoff were developed using the measured values, which were made prior to the first simulation and at the end of each simulation for each slope and replication. Relationships involving the measured flow velocities were identified using interpolated values of rock cover and roughness based on the timing of the velocity measurements relative to the timing of the rock cover and roughness measurements. The velocity measurements were made near the end of each simulation (plus toward the beginning of the first simulation), so the values of the rock cover and roughness were very nearly the same as the values measured at the end of each simulation (or prior to the first), but were adjusted slightly based on the measurements of rock cover and roughness that were made at the end of the previous simulation (or prior to the simulation, in the case of simulation 1.)

Calculations of random roughness was calculated as the standard deviation of all the trend-adjusted elevation measurements from the laser distance meter after removing 10 cm of data from the edges of the plot to remove plot edge effects.

3. Results

3.1 Rock Cover and Random Roughness Evolution

The initial rock covers for the 6 experiments ranged from 16 to 40%, and final covers ranged from 78 to 90% (Fig. 1). There was no relationship between the final rock cover and either the slope gradient (Table 1) or the initial rock cover (Fig. 1). Increasing the threshold size for defining "rock" from 0.5 cm to 1 and 2 cm did not change this result. There were also no trends in final rock cover as a function of the distance down the plot (Table 1), and there were no consistent trends in the rate of rock cover development as a function of downslope distance (Fig. 2). An example photo of rock cover taken after simulation 3 at 20% slope, replication 2 is shown in the supplementary material.

The final random roughness was quite different as a function of slope gradient treatments, with the steeper slopes resulting in a rougher final surface (Table 1; Fig. 3). There were no consistent differences in random roughness measured in the lower, middle, and upper sections of the plots (e.g., Fig. 4).

There were significant, but relatively weak, relationships between rock cover and random roughness (Fig. 5).

Table 1. Percentages of rock cover greater than 0.5 cm for the full, lower, middle, and upper portions of the plots, and laser-measured random roughness measured at the end of each experimental replication.

		Rock Cover				Random Roughness
Slope	Rep	Full	Lower	Middle	Upper	
%		%	%	%	%	mm
5	1	89	90	92	88	2.90
	2	80	81	76	81	3.04
12	1	85	80	89	84	4.39
	2	90	90	88	92	4.97
20	1	78	78	80	75	6.08
	2	88	90	89	85	6.29

3.2 Runoff Velocity and Hydraulic Friction Evolution

Measured runoff velocities tended to decrease as the slopes evolved to relatively consistent values of approximately 0.035 to 0.04 m s^{-1} at 59 mm hr^{-1} rainfall intensity, and 0.55 to 0.7 m s^{-1} at 178 mm hr^{-1} rainfall intensity (Fig. 6). Velocities on the evolved plots (at the end of each replication for each slope) were independent of slope gradient. The results support the hypothesis that flow velocities are dependent on overland flow unit discharge independent of slope gradient (Fig. 7), and the results fit a power relationship well:

$$v = 26.39\ q^{0.696}\ (r^2 = 0.95,\ n = 36) \quad (3)$$

where v is the average flow velocity (m s^{-1}) and q is the unit flow discharge across the plot (m^2 s^{-1}). Note that the flow variable used here is unit discharge, with units of (m^2 s^{-1}), rather than total discharge, which has units of (m^3 s^{-1}), which has been used in many previous studies of rill flow velocity.

Correspondent to the changes in runoff velocities, hydraulic friction factors indicated an increase in hydraulic roughness as the surfaces evolved (Fig. 8). By the time that cumulative runoff reached 1000 mm, according to the Chezy and Manning coefficients, the surfaces were hydraulically rougher on the steeper slopes (i.e., Chezy values were lesser and Manning values greater on steeper slopes compared to shallower slopes). Also, Chezy and Manning coefficients were different for the two rainfall intensities (and hence runoff rates), with lesser Chezy values and greater Manning values (e.g., apparently hydraulically rougher) for the lower rainfall and runoff rates. These results were statistically significant.

3.3 Hydraulic and Physical Surface Roughness

There were very clear and strong relationships between the hydraulic roughness coefficients (Manning and Chezy) and measured random roughness from the laser measurements taken at the end of each of the six replications (i.e., each replication for each of the 3 slopes) (Fig. 9). Both the random roughness and hydraulic roughness (as quantified by Chezy and Manning) were greater on the steeper slopes (Fig. 8, Table 1). Hydraulic resistance, as indexed by the roughness coefficients, was greater on physically rougher surfaces. These data (Figs. 8 and 9) show that the roughness coefficients were different for the two different rainfall rates, hence, there was not a unique hydraulic coefficient associated with a given surface roughness for these plots.

4 Discussion

Our results that show no dependence of final rock cover percentages, after the development of the erosion pavements, as a function of slope gradient (Fig. 1, Table 1) appear to contradict previous findings that indicate greater rock cover on steeper slopes. However, the final rock covers measured in this experiment are greater than those reported in previous work at Walnut Gulch, where the previous relationships were determined. Final rock covers in this experiment ranged from 78% to 90%, with an average of 85%. Rock covers measured by Simanton and Toy (1994) and Simanton et al. (1994) ranged from 2 to 77%. We conclude from these facts that the surfaces that evolved in this experiment were at maximum or near maximum coverage possible for this soil under natural hillslope conditions and climate of the area. A possible explanation for the somewhat lower rock cover values on the natural hillslopes may be related to factors at work that bring new material to the surface in the natural landscape, such as bioturbation and heaving associated with freeze/thaw, both of which are active in this and many other semi-arid landscapes (Emmerich, 2003).

Given the fact that rock cover did not vary with slope gradient, it is quite interesting that both random roughness of the surface (Fig.3, Table 1) and hydraulic roughness (Fig. 9) did so. This in fact is evidence of the development of slope-velocity-equilibrium. The steeper slopes evolved to both physically and hydraulically rougher surfaces compared to shallower slopes, even with similar rock covers, and in doing so maintained a constant relationship between flow velocities and unit discharge irrespective of slope (Fig. 7). We note that rainfall intensity also did not influence this unique relationship between velocity and discharge.

We are not sure yet exactly what process is taking place to effect the differences in roughness with slope independent of rock cover, but a corollary may be drawn to our understanding of flow rates in rills on non-rocky soils. Govers (1992), and Govers et al. (2000) reported on experiments with rills that showed a relationship between flow velocity and flow discharge independent of slope gradient on non-rocky soils. This was attributed largely to the development of headcuts (see also Rieke-Zapp et al., 2007; and Nearing et al. 1999). In our experiment it appears that development of greater form roughness occurred on the steeper slopes compared to the shallower slopes. One is tempted to compare the exponent determined from this experiment (Eq. 3) to exponents from previous work on rill flow velocities. However, it should be noted that Eq. 3 uses unit

width discharge while rill flow experiments typically reported relationships using total discharge (e.g., Eq. 2). Because of the complexity and variability in flow on interrill areas, it is not clear that a direct comparison of these values is entirely valid or robust. Nonetheless, under the specific conditions of this experiment, since width is a constant, then the use of total discharge for these data would also result in an exponent of 0.696 (see Eq. 3), though the equation would have a different linear coefficient. This is greater than values previously reported for rill studies, including a value of 0.294 determined by Govers (1992), 0.459 determined by Nearing et al. (1999), and 0.39 reported by Torri et al. (2012).

Our data are not inconsistent with the hypothesis that has been proposed for channel beds, that the feedback between bed morphology, erosion, and flow velocities is associated with, or controlled by the Froude number. Average Froude numbers calculated from the data tended to decrease as a function of the surface development, and stabilize toward the end of the replications. Average values of the Froude number were less than one in all but two cases, both of which were measured during the early stage of the experiments when the surface was just beginning to evolve to its final state (Figure 10). Of course there is no way using the data presented here to know the spatial variations in the Froude number occurring on the plot at any given time, nor where the Froude number may have approached unity. With detailed measurements of the surface morphology at various times during such an experiment as this, possibly combined with distributed measurements or modeling of the flow velocity field, it might be possible to better investigate the role of energy minimization and the Froude number threshold in the development of these types of surfaces and control of the runoff velocities.

The results of this study do not suggest that the overland flow relationships such as Chezy or Manning equations, are physically incorrect for flow modeling, but they do suggest that there are significant practical difficulties associated with their application to hillslope surfaces, which erode. Hydraulic friction factors, such as Chezy and Manning coefficients, are commonly used on runoff models for stony rangeland (and other) soils (Nouwakpo et al., 2016), but this usage is problematic because the coefficients depend on slope gradient and runoff rates, and hence with distance downslope on the hill and time during the runoff event. The data clearly showed that there was not a unique hydraulic coefficient for a given surface condition. Generally, Chezy and Manning roughness coefficients are presented in tables based on surface conditions, suggesting that they are not related to either slope or runoff rates. In order to accurately implement the use of these equations in models, the coefficients used should be adjusted for slope and runoff rates, which means that they should be adjusted both temporally and spatially on a hillslope within each runoff event.

The fact that there is a unique relationship between velocity and discharge would suggest that routing runoff over hillslopes in models using such a relationship (e.g., Fig. 7) would provide more consistent and realistic results. It would appear to be counterintuitive and convoluted to apply an equation that relates velocity to flow depths and slope when the coefficients in the equations used are dependent on slope, discharge rate, and physical roughness. As pointed out previously with respect to flow in rills, if we assume a constant roughness coefficient then "velocities will be over-predicted on steep slopes and under-predicted on shallower slopes" (Govers et al., 2000).

5 Summary and Conclusions

The results of this study are consistent with the hypothesis of slope-velocity-equilibrium as a state that evolves naturally over time due to the interaction between overland flow and bed surface morphology, wherein steeper areas develop a relative increase in surface and hydraulic roughness such that flow rates and velocities increase approximately linearly down the slope under normal runoff conditions, independent of slope gradient. If this were not the case, then either supercritical or backwater flow would occur, which would cause erosion or deposition to bring the slope into slope-velocity equilibrium.

Velocities were dependent on discharge rates alone. The relationship between velocity and discharge was independent of slope gradient or rainfall intensity.

Use of hydraulic friction factors, such as Chezy and Manning coefficients, are problematic because they depend on both slope and runoff rate. The data clearly showed that there is not a unique hydraulic coefficient for a given generalized surface condition.

References

Emmerich, W. E.: Season and erosion pavement influence on saturated soil hydraulic conductivity, Soil Sci., 168(9), 637-645, DOI: 10.1097/01.ss.0000090804.06903.3b, 2003.

Foster, G.R., Huggins, L.F. and Meyer, L.D.: A laboratory study of rill hydraulics: I. Velocity relationships. Trans. of the Am. Soc. Agric. Eng., 27(3), 790-796, 1984.

Govers, G.: Relationship between discharge, velocity and flow area for rills eroding loose, non-layered materials, Earth Surf. Processes and Landforms 17, 515–528, 1992.

Govers, G., Takken, I., and Helming, K.: Soil roughness and overland flow, Agronomie, 20, 131–146, 2000.

Graf, W. H.: Hydraulics of Sediment Transport, Water Resources Publications, Littleton, CO, 513pp, ISBN-0-918334-56-X. 1984.

Grant, G.E.: Critical flow constrains flow hydraulics in mobile-bed streams: A new hypothesis. Water Resources Research, 33(2), 349-358, 1997.

Hussein, M.H., Amien, I.M. and Kariem, T. H: Designing terraces for the rainfed farming region in Iraq using the RUSLE and hydraulic principles, Int. Soil and Water Conservation Res., 4(1), 39-44, 2016.

Lei, T., Nearing, M. A., Haghighi, K. and Bralts V.: Rill erosion and morphological evolution: A simulation model, Water Resources Res. 34(11), 3157-3168, 1998.

Nouwakpo, S. K., Williams, C. J., Al-Hamdan, O., Weltz, M. A., Pierson, F, Nearing, M. A.: A review of concentrated flow erosion processes on rangelands: fundamental understanding and knowledge gaps, Int. Soil and Water Conservation Res., 4(2), 75-86, 2016.

Nearing, M.A., J.R. Simanton, L.D. Norton, S.J. Bulygin, and J. Stone: Soil erosion by surface water flow on a stony, semiarid hillslope. Earth Surface Processes and Landforms 24:677-686, 1999.

Nearing, M. A., Norton, L. D., Bulgakov, D. A., Larionov, G. A., West, L. T., and Dontsova, K. M.: Hydraulics and erosion in eroding rills. Water Resources Res. 33(4), 865-876, 1997.

Nearing, M. A., Norton, L. D., Zhang, X.: Soil erosion and sedimentation, in: Agricultural Nonpoint Source Pollution, W.F. Ritter and A. Shirmohammadi (eds.), Lewis Publishers, Boca Raton, 29-58, ISBN 1-56670-222-4, 2001.

Nearing, M. A., Kimoto, A., Nichols, M. H., and Ritchie, J. C.: Spatial patterns of soil erosion and deposition in two small, semiarid watersheds, J. Geophys. Res., 110, F04020, doi:10.1029/2005JF000290, 2005.

Paige, G. B., Stone, J. J., Smith, J. R. and Kennedy, J. R.: The Walnut Gulch rainfall simulator: A computer-controlled variable intensity rainfall simulator, Applied Engineering in Agric., 20(1), 25-34, 2004.

Poesen, J. W., van Wesemael, B., Bunte, K., and Benet A.: Variation of rock cover size along semi-arid hillslopes: a case study from Southeast Spain. Geomorphology, 23, 323-335, 1998.

Rieke-Zapp, D. H., Poesen, J., and Nearing, M. A.: Effects of rock fragments incorporated in the soil matrix on concentrated flow hydraulics and erosion, Earth Surface Processes and Landforms, 32, 1063-1076, 2007.

Shaw, C. F.: Erosion Pavement. Geographical Review 19(4). 638-641, 1929.

Simanton, J. R., and Toy, T. J.: The relation between surface rock fragment cover and semiarid hillslope profile morphology. Catena. 23, 213-225, 1994.

Simanton, J. R., Renard, K. G., Christiansen, C. M., and Lane, L. J.: Spatial distribution of surface rock fragments along catenas in semiarid Arizona and Nevada, USA. Catena, 23, 29–42, 1994.

Stone, J. J. and Paige, G. B.: Variable rainfall intensity rainfall simulator experiments on semi-arid rangelands, Proc. 1st Interagency Conf. on Res. in the Watersheds, Benson, AZ, USA. 27-30 Oct., 2003, 83-88, 2003.

Takken, I., Govers, G., Ciesiolka, C. A. A., Silburn, D. M. and Loch, R. J.: Factors influencing the velocity-discharge relationship in rills, in: Modelling Soil Erosion, Sediment Transport and Closely Related Hydrological Processes, IAHS Publ. no. 249, 63-70, 1998.

Torri, D., Poesen, J., Borselli, L., Bryan, R. and Rossi, M.: Spatial variation of bed roughness in eroding rills and gullies. Catena, 90, 76-86, 2012.

vanWesemael, B., Poesen, J. deFigueiredo, T., Govers, G.: Surface roughness evolution of soils containing rock fragments, Earth Surface Processes and Landforms, 21(5), 399-411, DOI: 10.1002/(SICI)1096-9837(199605)21:5<399::AID-ESP567>3.0.CO;2-M, 1996.

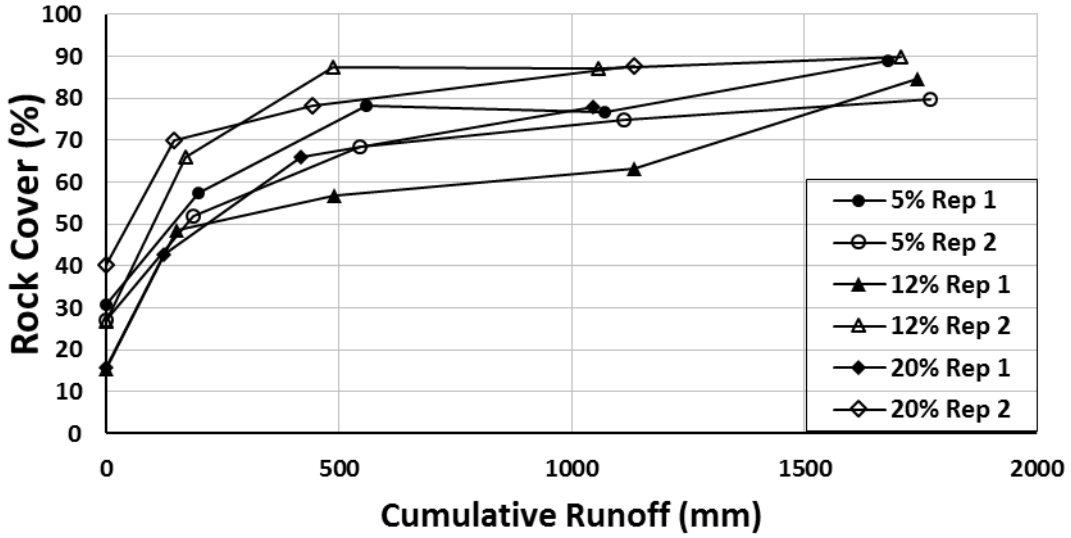

Figure 1. Plot-average rock cover (>0.5 cm) as a function of cumulative runoff for the 6 experiments.

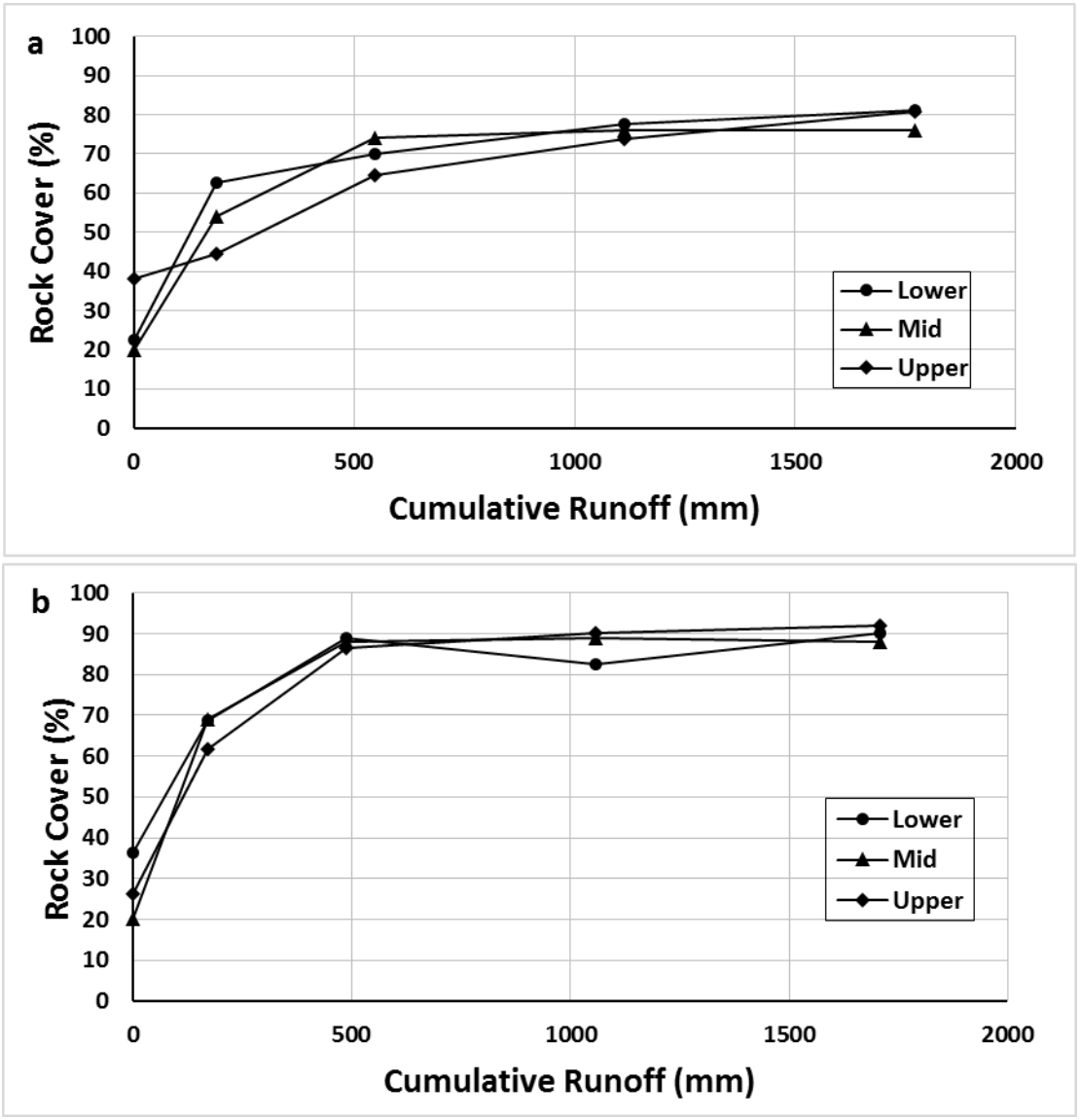

Figure 2. Surface rock cover (>5 mm) on the three sections of the plots as a function of cumulative runoff for: a) 5% slope, replication 2; and b) 12% slope, replication 2.

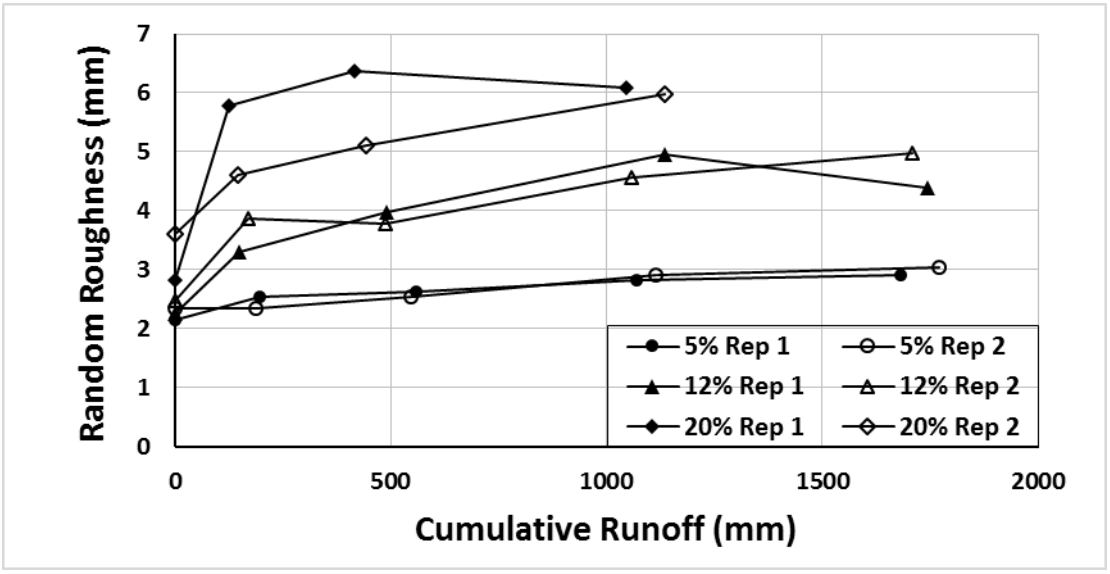

Figure 3. Averages of the three cross-section (lower, middle, and upper) laser-measured random roughness measurements (mm) as a function of cumulative runoff for the six experiments.

5

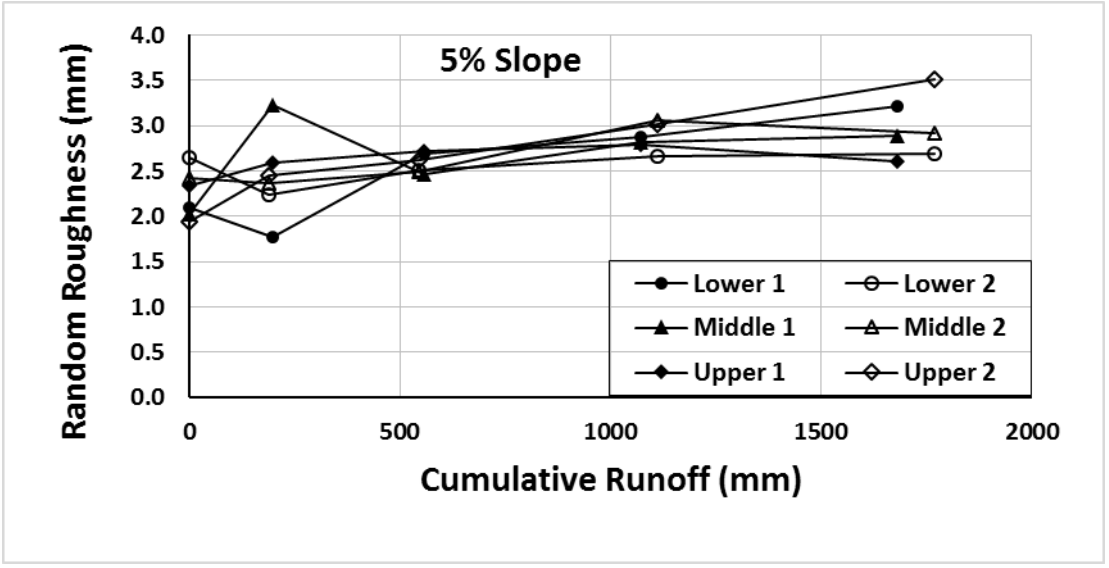

Figure 4. Laser-measured random roughness measurements (mm) at the three cross-sections (lower, middle, and upper) as a function of cumulative runoff at 5% slope, replications 1 and 2.

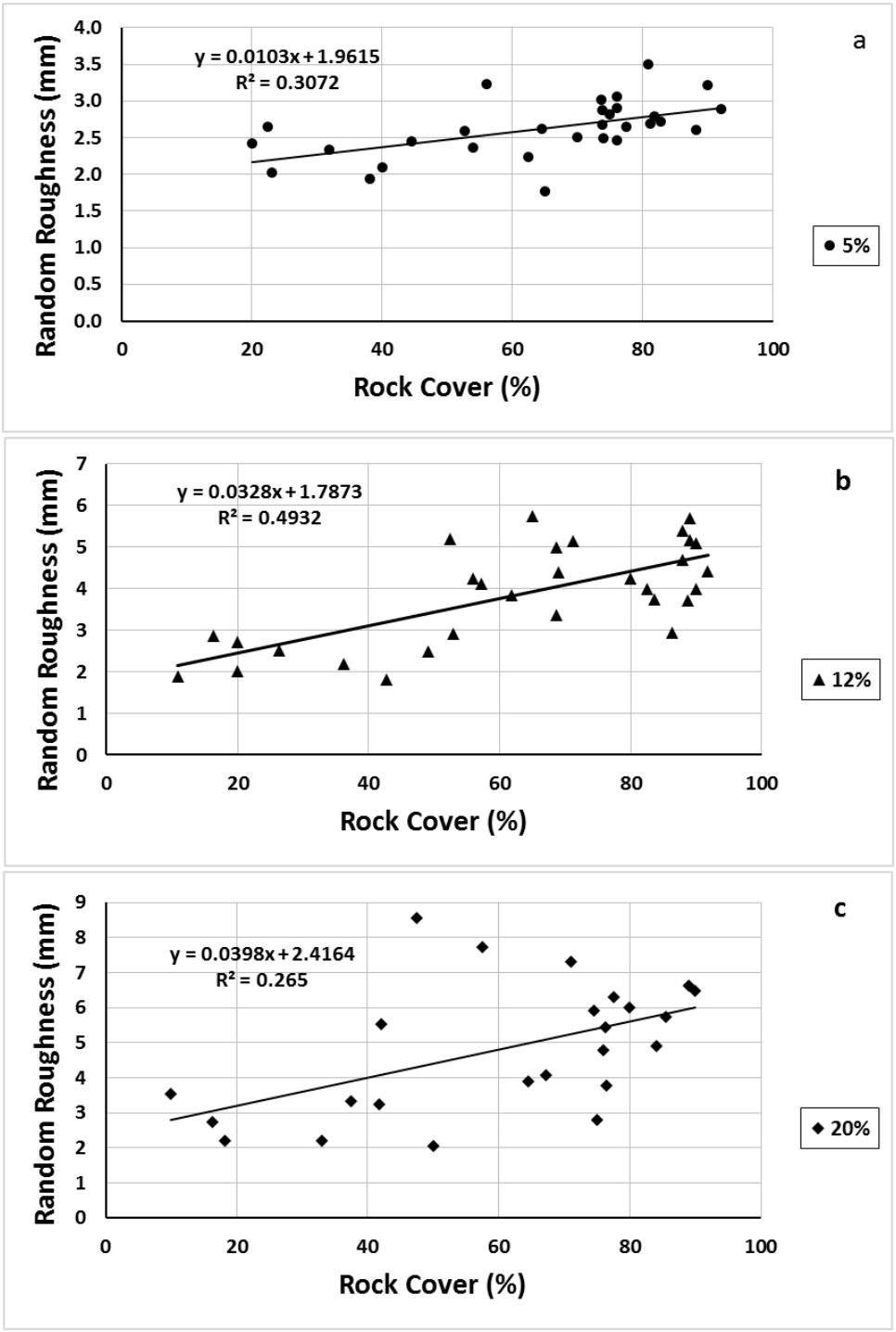

Figure 5. Random roughness as a function of rock cover on all sections of the plots and both replications for a) 5%, b) 12%, and c) 20% slope gradients.

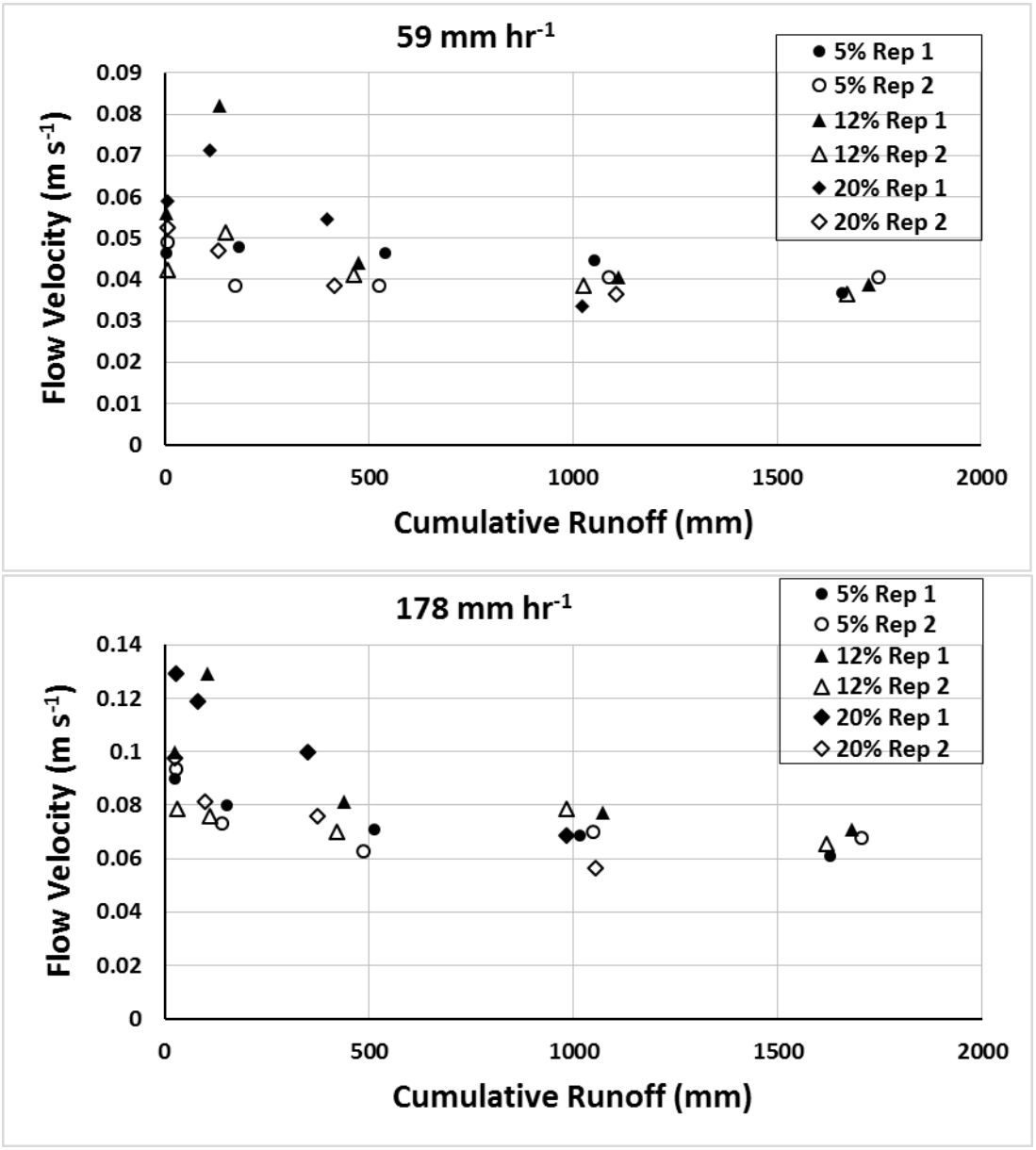

Figure 6. Flow velocities down the full plot as a function of cumulative runoff depth for: a) I=59 mm hr^{-1}, and b) I=178 mm hr^{-1}.

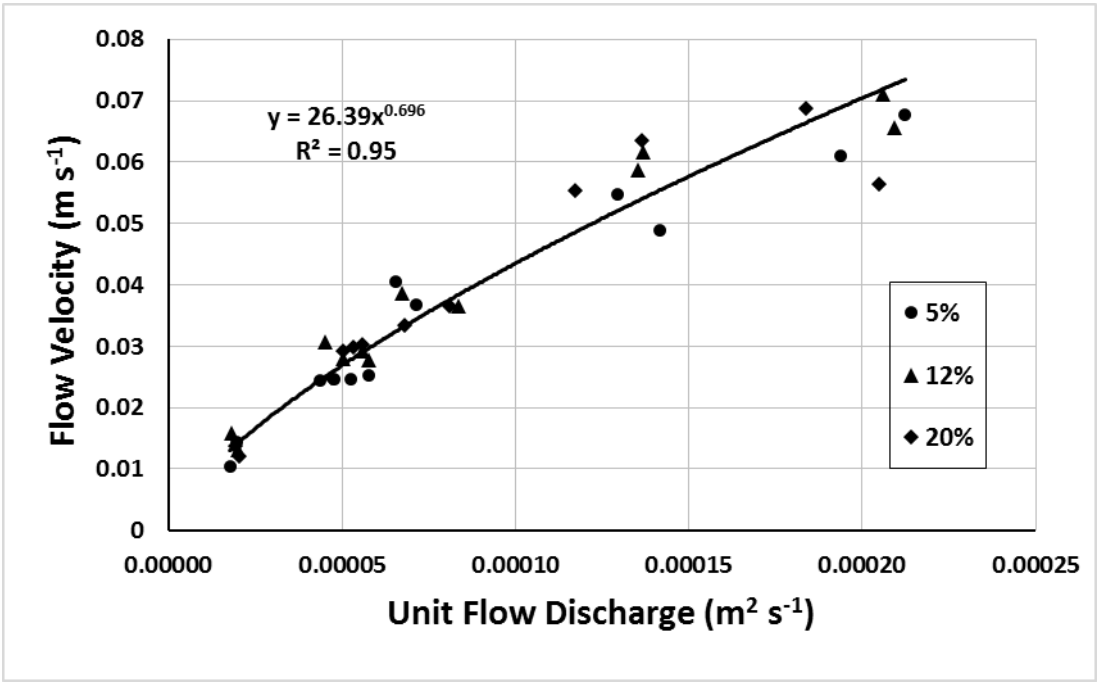

Figure 7. Final flow velocities for all 6 experiments at each of the three velocity transect measurement transects and two rainfall rates.

5

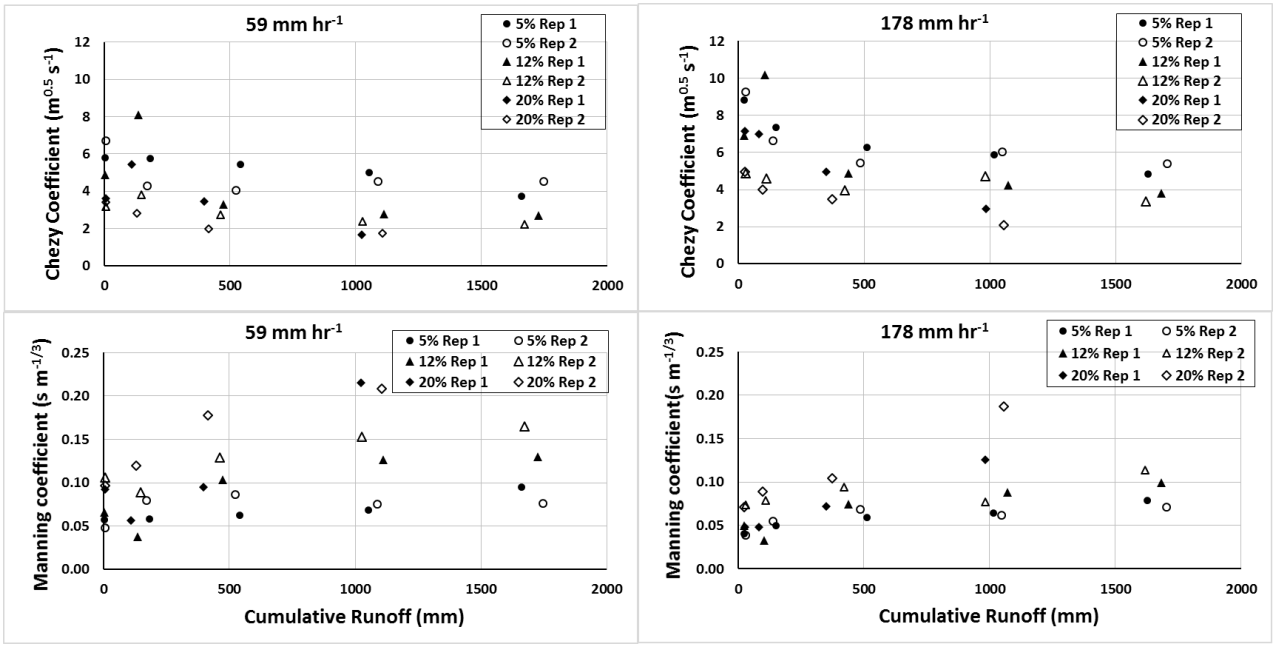

Figure 8. Hydraulic friction factors, Chezy and Manning coefficients, for full length of the plots as a function of cumulative runoff for 59 and 178 mm hr^{-1} rainfall intensities.

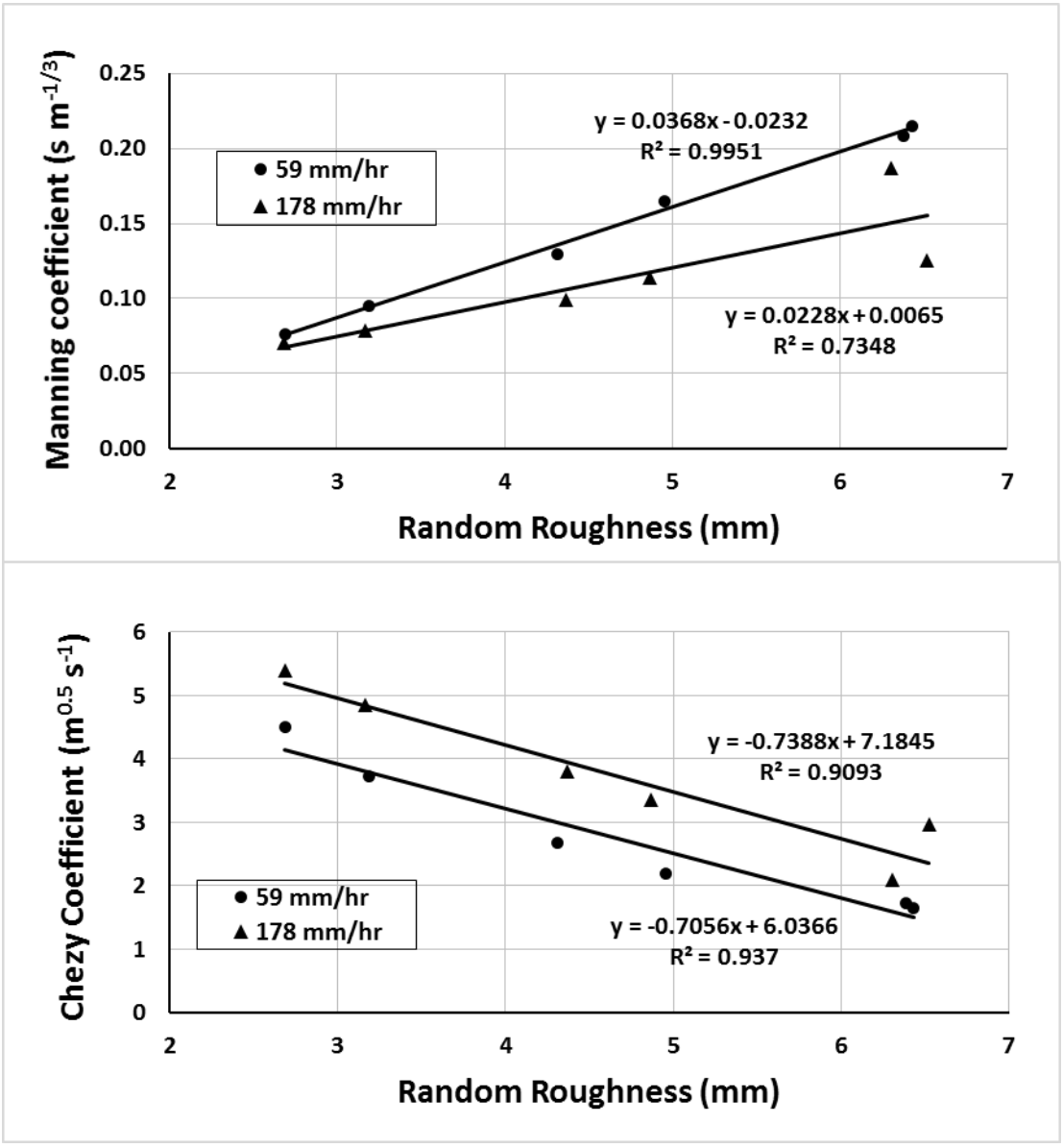

Figure 9. Relationships between the roughness coefficients, Chezy and Manning, to laser measured random roughness.

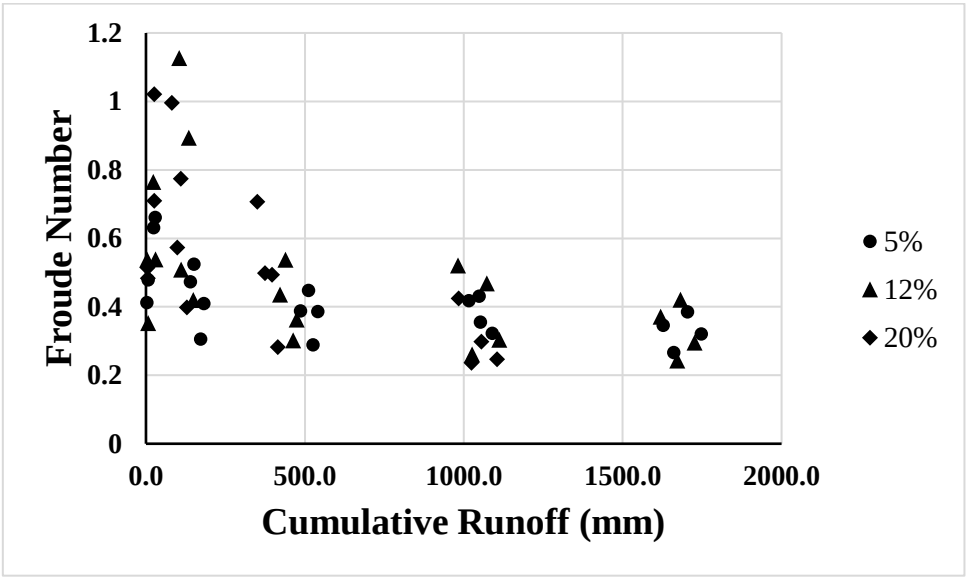

Figure 10. Froude Number based on full plot length velocity and flow measurements.